Materials Science Forum
ISSN: 1662-9752, Vol. 1182, pp 1-11
doi:10.4028/p-aI6KaL

Submitted: 2025-12-19
Revised: 2026-02-11
Accepted: 2026-02-14
Online: 2026-04-10

Validation of Thermoforming Simulation Models Prior to Parameterization Using Covariance-Based Input-Output Statistics – Assessing the Role of Thermomechanical Material Modeling

Johannes Mitsch[a*], Tobias Würth[b], Jan Paul Wank[c], and Luise Kärger[d]

Karlsruhe Institute of Technology (KIT), Institute of Vehicle System Technology (FAST) – Lightweight Engineering, 76131 Karlsruhe, Germany

[a]Johannes.Mitsch@kit.edu,[b]Tobias.Wuerth@kit.edu, [c]Jan.Wank@kit.edu, [d]Luise.Kaerger@kit.edu

Keywords: Forming, Process Simulation, Finite Element Analysis (FEA), Validation Techniques

Abstract. Accurate yet computationally efficient simulation models are essential for the virtual design and optimization of thermoforming processes for fiber-reinforced composites. Selecting an appropriate material model remains challenging, particularly when balancing model fidelity against computational cost. In this work, a framework is developed to validate material models used in thermoforming simulations for fiber-reinforced composites. The framework evaluates model performance based on time-series data using covariance-based input-output statistics, without prior calibration. Two numerical studies of increasing complexity demonstrate the versatility of the approach. First, the framework is applied to one-dimensional rheological models, verifying its applicability to mechanical problems relevant to thermoforming simulation. These insights are then applied to complex finite element thermoforming simulations to assess the ability of isothermal material models to predict wrinkling behavior in comparison to a fully coupled thermomechanical reference model. A curvature-based method is introduced to quantitatively evaluate wrinkling severity relative to natural curvatures induced by the tool geometry. The results show that isothermal models are sufficient for short total process times with minor temperature-driven effects, whereas longer total process times with pronounced thermal effects require thermomechanical models to ensure accurate predictions. The findings offer practical guidance for selecting appropriate material models based on specific process conditions, as well as objective criteria for assessing model validity in virtual process design.

1. Introduction

In numerical model development, the goal is to create mathematical representations that capture experimentally observed phenomena and accurately predict system behavior while maintaining computational efficiency. In virtual process design for fiber-reinforced composites, this balance is particularly important due to the need for rapid simulations that support design and process optimization. With the growing number of modeling approaches for composite forming [1], systematic strategies for model selection and validation are increasingly required to determine when simplified models are sufficient and when higher-fidelity approaches are necessary.

Traditional model validation is typically performed after calibration by comparing model predictions point-wise to independent experimental data. However, calibration errors can obscure fundamental modeling deficiencies and compromise the validity of the results [2]. To address this issue, Vogel and Sankarasubramanian [2] proposed a model validation framework for watershed models that separates calibration from validation. Rather than relying on point-by-point agreement, the framework evaluates whether the model reproduces the underlying system dynamics by comparing input and output time series and their statistical dependencies. These dependencies are assessed over an ensemble of simulations with varying model parameters to explore the system's dynamic behavior and compare it systematically to reference data. Unlike traditional validation approaches, the framework is not able to confirm model validity with certainty but can reject models that fail to reproduce the system dynamics adequately. While it has been successfully applied in hydrological modeling [3], its use in mechanical problems, particularly forming simulations of composite materials, remains largely unexplored.

The objective of this work is to adapt and apply the model validation framework originally proposed by Vogel and Sankarasubramanian [2] to thermoforming simulations of fiber-reinforced composites. The framework is first tested on simplified one-dimensional rheological models to demonstrate its applicability to mechanical problems relevant to thermoforming. The insights gained are then used to extend the framework to complex finite element simulations for thermoforming of composite materials. Finally, the validation approach is applied to systematically compare the performance of isothermal [4] and thermomechanical [5] material models, providing insights into the role and necessity of thermomechanical coupling in forming simulations.

2. Numerical Study on One-Dimensional Rheological Models

Material models. To demonstrate the applicability of the proposed validation framework to mechanical models used in thermoforming simulations, two simplified one-dimensional (1D) rheological models are considered: a standard (isothermal) Voigt-Kelvin model and a thermomechanical Voigt-Kelvin model. The standard Voigt-Kelvin model consists of a spring and a damper connected in parallel. The constitutive equation of the isothermal Voigt-Kelvin model is given by

$$\sigma(t) = E\varepsilon(t) + \eta\dot{\varepsilon}(t), \tag{1}$$

where $\sigma(t)$ is the stress, $\varepsilon(t)$ the strain, E the elastic modulus and η the viscosity. The thermomechanical Voigt-Kelvin model extends this formulation by including thermal expansion in the spring element. The constitutive equation of the thermomechanical Voigt-Kelvin model is given by

$$\sigma(t) = E\left(\varepsilon(t) - \alpha\left(T(t) - T_0\right)\right) + \eta\dot{\varepsilon}(t), \tag{2}$$

where α is the thermal expansion coefficient, $T(t)$ the current temperature, and T_0 a reference temperature. The input-output behavior of both models is illustrated in Fig. 1 for a given stress input $\sigma(t)$, temperature profile $T(t)$, and reference parameter set (cf. Table 1). The stress input and strain output are normalized between 0 and 1 for comparability. As expected, the thermomechanical model's response varies with temperature, whereas the isothermal model remains unaffected. This substantial difference in model behavior will be used to demonstrate the validation framework.

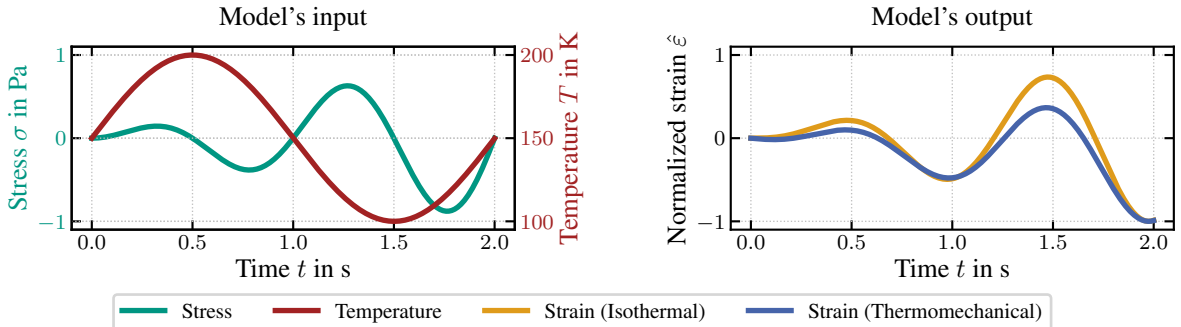

Fig. 1: In- and output time series of the variotherm and isotherm Voigt-Kelvin models.

Experimental setup and material parameters. To apply the validation framework, both models are simulated under identical input conditions, specifically the time-dependent stress input $\sigma(t)$ and the temperature profile $T(t)$ shown in Fig. 1 (left). A total of 4000 simulations are performed for each model, with material parameters varied to comprehensively assess the performance of the validation framework. The parameters are sampled using Latin Hypercube Sampling (LHS) [6] to ensure a well-distributed exploration of the parameter space. Parameters spanning more than one order of magnitude are sampled on a logarithmic scale. A summary of the sampled parameter ranges is provided in Table 1.

Table 1: Parameter ranges for the LHS of the 1D rheological models

Description	Symbol	Reference	Range	Unit	Log-scaling
Elastic modulus	E	10^2	$[10^1, 10^4]$	MPa	Yes
Viscosity	η	10^2	$[10^1, 10^4]$	MPa · s	Yes
Thermal expansion coefficient	α	$5 \cdot 10^{-6}$	$[10^{-9}, 10^{-4}]$	$1/\mathrm{K}$	Yes
Reference temperature	T_0	250	$[100, 500]$	K	No

Note that, in reality, material parameters such as the elastic modulus E and viscosity η can be temperature-dependent. This effect is neglected here for simplicity and to isolate the influence of temperature on the thermal expansion coefficient α.

Covariance-based validation metrics. To apply the validation framework of Vogel and Sankarasubramanian [2] to the 1D rheological models, the variance $\mathrm{Var}(f)$ and the Pearson correlation coefficient $\rho(f, g)$ between two discrete time series f and g are used as covariance-based validation metrics. The variance $\mathrm{Var}(\cdot)$ quantifies the spread of a time series around its empirical mean value $\bar{(\cdot)}$

$$\mathrm{Var}(f) = \frac{\sum_{i=1}^{N_t} \left|(f(t_i) - \bar{f})^2\right|}{N_t} \quad \text{with the empirical mean value} \quad \bar{f} = \frac{1}{N_t} \sum_{i=1}^{N_t} f(t_i), \tag{3}$$

where N_t denotes the number of discrete time steps t_i. The Pearson correlation coefficient $\rho(f, g)$ measures the linear relationship between two time series

$$\rho(f, g) = \frac{\mathrm{Cov}(f, g)}{\sqrt{\mathrm{Var}(f)}\sqrt{\mathrm{Var}(g)}} = \frac{\sum_{i=1}^{N_t}(f(t_i) - \bar{f})(g(t_i) - \bar{g})}{\sqrt{\mathrm{Var}(f)}\sqrt{\mathrm{Var}(g)}}, \tag{4}$$

where $\mathrm{Cov}(f, g)$ denotes the covariance between f and g.

Vogel and Sankarasubramanian [2] originally proposed using the lag-one autocorrelation instead of the variance $\mathrm{Var}(f)$, which is equivalent to the Pearson correlation of a time series with a one-step time lag $\rho(f, f_{\mathrm{lag}})$.This captures the correlation of a time series with its immediate past values. Since the output time series of the 1D rheological models do not exhibit rapid fluctuations between consecutive time steps, the variance $\mathrm{Var}(f)$ is adopted here as a more suitable metric to quantify the spread of the time series.

Results and discussion. The validation metrics defined in Eq. 3 and Eq. 4 are computed for all 4000 parameter sets of both the isothermal (Eq. 1) and thermomechanical (Eq. 2) Voigt-Kelvin models using the stress $\sigma(t)$ and temperature $T(t)$ time series as inputs and the resulting normalized strain $\hat{\varepsilon}(t)$ time series as outputs. The results are shown in Fig. 2, where each point represents a simulation with a specific parameter set. Orange and blue points correspond to the isothermal and thermomechanical models, respectively, while green markers highlight the reference parameter set (E, η, T_0) from Table 1 where the thermal expansion coefficient α is varied.

In both plots of Fig. 2, the points of the isothermal model (orange) form a subset of those of the thermomechanical model (blue), as the former represents a special case of the latter with $\alpha = 0$. The thermomechanical simulations highlighted in green, where only α is varied, form a curve within the thermomechanical model's point cloud and approach the isothermal points as α approaches small values. This indicates that for small thermal expansion coefficients α, the system dynamics of the thermomechanical model converge to those of the isothermal model. According to the validation framework [2], the isothermal model should be rejected as an invalid simplification when the value of α is large, since this simplified model does not capture the significant influence of temperature on system dynamics. However, for small α values, the isothermal model might still be considered valid if the material parameters are chosen appropriately. It should be noted that individual locations in the

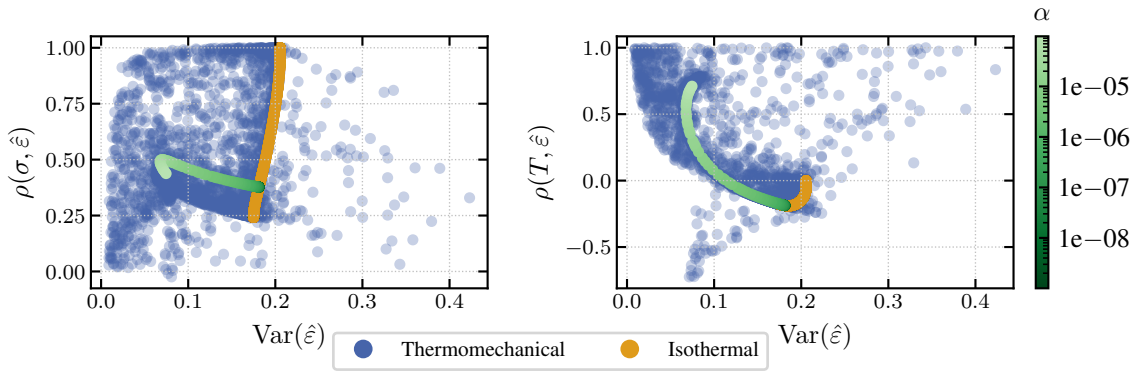

Fig. 2: Evaluation of validation metrics across thermal expansion coefficients α, comparing isothermal and thermomechanical Voigt-Kelvin models. Left: stress-strain correlation vs. strain variance. Right: temperature-strain correlation vs. strain variance

covariance-based metric space cannot be uniquely interpreted in terms of specific material parameters, as the framework evaluates system-level dynamic behavior rather than parameter-wise effects.

These results confirm that the covariance-based metrics (variance and Pearson correlation) are suitable for evaluating mechanical material models. Finally, Fig. 2 also shows that using normalized input and output time series produces a well-distributed point cloud, confirming that normalized input and output time-series are preferable for the covariance-based validation framework. The one-dimensional study therefore serves as a methodological verification step, demonstrating that the covariance-based framework can be meaningfully transferred from hydrological [2] to mechanical modeling contexts.

3. Adaption and Application to Thermoforming Simulation

Approach. To apply the validation framework proposed by Vogel and Sankarasubramanian [2] to finite element simulations of thermoforming composite materials, two material models of different complexities are employed. A state-of-the-art, fully coupled, high-fidelity thermomechanical simulation model is used as a reference. It serves as a substitute for experimental data. A lower-fidelity, isothermal simulation model is evaluated based on its ability to reproduce the input-output behavior of the reference model's wrinkling response. Both models are implemented in the commercial finite element software Abaqus/Explicit and are based on the works of Dörr et al. [4, 5]. The validation framework is applied to investigate the necessity of considering thermomechanical coupling in forming simulations of thermoplastic composite materials based on the wrinkling behavior during forming. To quantify the severity of wrinkling during forming as a time series, a quantitative metric, based on the Wrinkled Element Ratio (r_w) [7], is introduced as the output time series for the validation framework.

Material modeling. The lower-fidelity simulation is based on the work of Dörr et al. [4], who developed an isothermal thermoforming simulation approach for thermoplastic composite materials, neglecting temperature-driven phenomena during forming. Superimposed two-dimensional membrane (M3D3) and shell (S3) element formulations with VUMAT and VUGENS user subroutines are employed. This allows for a decoupled description of the membrane and bending behavior in each individual ply [4]. Both the membrane and bending behaviors are modeled using an isothermal Voigt-Kelvin material model

$$\boldsymbol{S}^{\mathrm{2PK}} = \boldsymbol{S}^{\mathrm{2PK}}_{\mathrm{elast}} + \boldsymbol{S}^{\mathrm{2PK}}_{\mathrm{visc}} \tag{5}$$

employing a hyperelastic St. Venant-Kirchhoff model for the elastic part,

$$\boldsymbol{S}^{\mathrm{2PK}}_{\mathrm{elast}} = \mathbb{C}[\boldsymbol{E}], \tag{6}$$

while the viscous behavior is described by an isotropic Newton model with a nonlinear Cross approach for the viscosity [4],

$$\boldsymbol{\sigma}_{\mathrm{visc}} = \eta(\dot{\gamma})\boldsymbol{D} \quad \text{with} \quad \eta(\dot{\gamma}) = \frac{\eta_0}{1 + (m\dot{\gamma})^{1-n}}. \tag{7}$$

The inter-ply behavior is modeled according to the isotropic approach of Dörr et al. [8], accounting for non-penetration, adhesion, and sticking-sliding interactions between adjacent plies. A detailed description of the isothermal forming simulation model is provided in the original publications [4, 8].

The high-fidelity thermomechanical reference simulations are based on the work of Dörr et al. [5], who developed a fully coupled thermomechanical forming simulation approach for thermoplastic composite materials. Unlike the isothermal model, this model also accounts for temperature-dependent material behavior, tool-ply and ply-ply heat transfer, crystallization kinetics, and the phase transitions between the molten and solid states of the thermoplastic matrix during cooling. Similar to the lower-fidelity model, the simulation is implemented in Abaqus/Explicit using triangular membrane (M3D3) and shell (S3) element formulations with VUMAT and VUGENS subroutines for a decoupled description of the membrane and bending behavior in each ply. Heat transfer and crystallization kinetics are modeled using an additional layer of superimposed triangular elements in combination with VUEL and VUFIELD subroutines. The resulting temperature T and crystallization degree χ fields are then transferred into the VUMAT and VUGENS subroutines, enabling a temperature-dependent material description of the molten matrix material (cf. Eq. 6 and Eq. 7)

$$\mathbb{C}^{\mathrm{m}} = \mathbb{C}^{\mathrm{m}}(T) \quad \text{and} \quad \eta_0^{\mathrm{m}} = \eta_0^{\mathrm{m}}(T). \tag{8}$$

The phase transition between the molten and solid states of the thermoplastic material is modeled using a linear mixture rule based on the degree of crystallinity χ and the mechanical properties of the molten $(\cdot)^{\mathrm{m}}$ and solid $(\cdot)^{\mathrm{s}}$ states

$$\boldsymbol{S}^{\mathrm{2PK}}(T, \chi) = (1 - \chi)\boldsymbol{S}^{\mathrm{m}}(T) + \chi\boldsymbol{S}^{\mathrm{s}}. \tag{9}$$

A more comprehensive description of the high-fidelity thermoforming simulation model is provided by Dörr et al. [5].

Experimental simulation setup and material parameters. For both simulation approaches, the same complex shaped tool geometry with the same spatial mesh resolution is used. The spatial discretization of the 410×410 mm sized blank consists of 6724 triangular elements for both simulation models and has an initial thickness of $d = 0.16$ mm per ply. The blank is initially situated between the forming tools. A biaxial laminate stack of $[0°, 90°]$ is selected to avoid wrinkling phenomena caused by complex stacking sequences, which could obscure wrinkling induced by temperature-driven effects. The forming process is executed by moving the forming tool downwards to shape the blank into the tool geometry. A smoothed tool displacement $u_{\mathrm{tool}}(t)$ profile is used for all simulations. Four different tool closing velocities with total process times t_{u} ranging from $1.6\,\mathrm{s}$ to $6.4\,\mathrm{s}$ are simulated. Longer total process times t_{u} increase the influence of temperature-driven phenomena on the forming result, as they lead to more cooling of the blank during forming and thereby raise the necessity to consider temperature-driven phenomena for accurate simulation [9].

For the high-fidelity thermomechanical forming simulations, a uniform initial blank temperature of $T_0 = 280°\mathrm{C}$ and a constant tool temperature of $T_{\mathrm{tool}} = 80°\mathrm{C}$ are selected, representing typical industrial forming conditions for the thermoplastic composite material used in this study [10]. The material parameters required for the thermomechanical simulations are obtained from in-house mechanical and thermal characterization tests of unidirectional carbon fiber reinforced polyamide composite material

[5]. In the four high-fidelity reference simulations, all material parameters are kept constant, and only the process time $t_\mathrm{u} \in \{1.6\,\mathrm{s}, 3.2\,\mathrm{s}, 4.8\,\mathrm{s}, 6.4\,\mathrm{s}\}$ is varied. For the lower-fidelity model, eight material parameters defining the isothermal material models for both the membrane and bending behavior are varied within physically reasonable ranges. The parameter ranges are obtained by means of an in-house database of material parameter sets for various material systems, with different matrix and fiber materials. Parameters varying over more than one order of magnitude are sampled in logarithmic space to ensure a uniform distribution across their range. A summary of the varied parameters and their ranges is given in Table 2. In total 1000 isothermal forming simulations are performed for each process time t_u using different parameter sets.

Table 2: Varied material parameters of the isothermal material models used in the lower-fidelity forming simulation. The resulting simulation data is provided by Mitsch and Kärger [11].

Material model	Description	Parameter	Range	Unit	Log-scaling
Membrane	Matrix elasticity	E^M	$[10^{-3},\, 10^{-1}]$	MPa	Yes
	Zero-strain viscosity	η_0^M	$[8 \cdot 10^{-3},\, 8 \cdot 10^{-1}]$	MPa·s	Yes
	Time constant	m^M	$[10^{-1},\, 5 \cdot 10^{1}]$	s	Yes
	Shear-thinning index	n^M	$[-1,\, 1]$	-	No
Bending	Flexural modulus 0°	C_{11}^B	$[3 \cdot 10^{1},\, 6 \cdot 10^{2}]$	MPa	Yes
	Zero-strain viscosity	η_0^B	$[1 \cdot 10^{0},\, 7 \cdot 10^{3}]$	MPa·s	Yes
	Time constant	m^B	$[1 \cdot 10^{-1},\, 5 \cdot 10^{7}]$	s	Yes
	Shear-thinning index	n^B	$[-1,\, 1]$	-	No

Note that under the assumption of negligible Poisson's ratio effects in the membrane ($\nu^\mathrm{M} = 0$), the membrane shear modulus G^M can be directly derived from the Young's modulus E^M of the matrix material as $G^\mathrm{M} = 1/2\, E^\mathrm{M}$. Furthermore, the flexural modulus in the $90°$ direction C_{22}^B and the flexural shear modulus G_{12}^B are derived from C_{11}^B using knock-down factors of $k_{22} = 100 = C_{11}^\mathrm{B}/C_{22}^\mathrm{B}$ and $k_{12} = 200 = C_{11}^\mathrm{B}/G_{12}^\mathrm{B}$ [4].

Generation of input and output time series for thermoforming simulation. In order to apply the proposed validation framework [2] to forming simulations, one time series defining the model's input and one time series defining the model's output must be extracted from the simulation data. For the input time series, the relative tool stroke Δu is chosen, defined as the displacement of the forming tool u_tool normalized by the maximum tool displacement u_max

$$\Delta u = u_\mathrm{tool}/u_\mathrm{max}. \tag{10}$$

As the output time series, the wrinkled element ratio r_w originally proposed by Chen et al. [7] is used to quantify the amount of wrinkling occurring during the forming process. The wrinkled element ratio r_w is defined as the area-weighted ratio of the number of wrinkled elements N_w to the total number of elements N_tot on the blank

$$r_\mathrm{w} = \frac{A_\mathrm{w}}{A_\mathrm{tot}} = \frac{\sum_{i=1}^{N_\mathrm{w}} A_i}{\sum_{j=1}^{N_\mathrm{tot}} A_j} = \frac{\sum_{i=1}^{N_\mathrm{tot}} w_i A_i}{\sum_{j=1}^{N_\mathrm{tot}} A_j} \quad \text{with} \quad w_i = \begin{cases} 1, & \text{if element } i \text{ is wrinkled,} \\ 0, & \text{else.} \end{cases} \tag{11}$$

A finite element is classified as wrinkled ($w_i = 1$) if its absolute curvature $|\kappa_i|$ exceeds a threshold curvature κ_crit. The curvature κ_i is calculated based on the node coordinates using the methodology proposed by Dong and Wang [12]. Note, that both quantities Δu and r_w are naturally normalized to the range $[0, 1]$ which was found to be beneficial for the application of the validation framework to the 1D rheological models above.

To objectively evaluate r_w for different tool geometries and process parameters, the threshold curvature κ_{crit} must be defined. In this work, κ_{crit} is defined as the 95th percentile of the curvature distribution of the blank mesh projected onto the tool geometry. This approach ensures, that the natural curvature induced by the tool geometry is used as a baseline for defining wrinkled elements while also accounting for the specific mesh resolution of the blank. The 95th percentile is selected to mitigate the influence of numerical noise and local mesh imperfections that may create small regions of artificially high curvature. This methodology enables an objective and consistent definition of wrinkled elements across different forming geometries. Note that the proposed method depends on the mesh resolution. Therefore, a consistent mesh resolution must be ensured when comparing r_w values across different simulations and when defining κ_{crit}.

A visualization of the r_w is shown in Fig. 3a, where wrinkled elements are highlighted in red and non-wrinkled elements in light gray. The selected threshold curvature κ_{crit} effectively separates wrinkled from non-wrinkled regions, demonstrating that this approach can quantitatively describe the amount of wrinkling in formed parts. As a global metric, however, r_w aggregates wrinkling information over the entire part and does not capture the spatial distribution of wrinkles. Some highly curved regions caused by the tool geometry are also partially classified as wrinkled due to the chosen thresholding approach, which is a trade-off between neglecting artificial numerical noise using the 95th percentile threshold and capturing genuine wrinkling phenomena. Since this effect is consistent across all simulations, it does not affect the comparative assessment of wrinkling behavior.

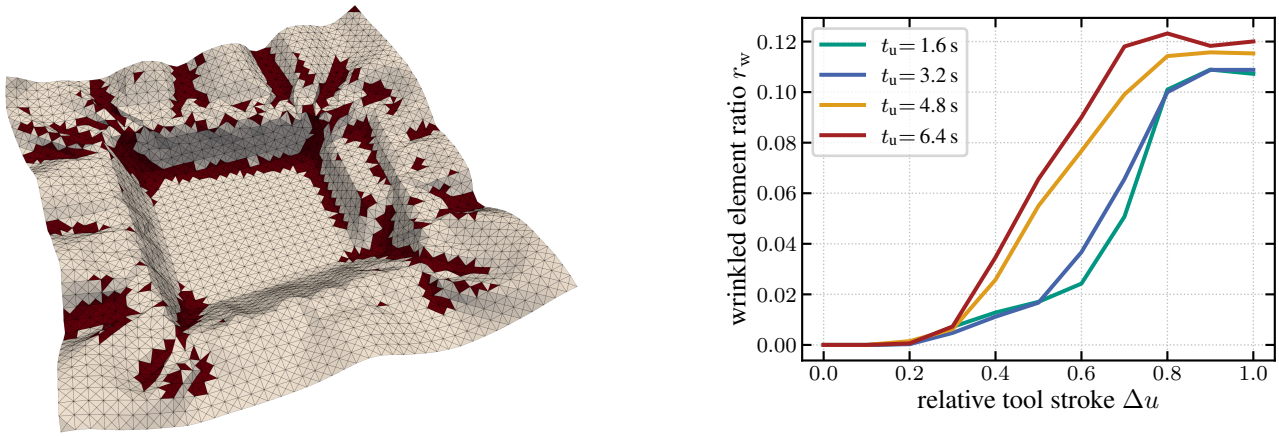

(a) (b)

Fig. 3: Quantitative assessment of the degree of wrinkling in forming simulations. (a) Visualization of wrinkled elements in red. (b) r_w curves for different total process times t_u in thermomechanical forming simulations.

The results of the r_w evaluation for the high-fidelity thermomechanical forming simulations with different total process times t_u are shown in Fig. 3b. In all cases, r_w increases during forming, indicating progressive wrinkle formation as the blank conforms to the tool geometry. It also rises more rapidly with increasing total process time t_u, suggesting that longer processes promote stronger wrinkling. This trend can partly be attributed to cooling effects at longer total process times t_u, which increases the material's viscosity and stiffness during forming [9] and contribute to crystallization effects (cf. Eq. 8 and Eq. 9). However, longer total process times t_u also reduce deformation rates, further increasing viscosity due to the shear-thinning behavior of the thermoplastic matrix material (Eq. 7). Thus, the observed wrinkling behavior results from the combined influence of thermomechanical coupling and deformation-rate effects.

Results and discussion of the validation framework. In order to apply the validation framework [2] to thermoforming simulation, four high-fidelity thermomechanical forming simulations at different total process times $t_\mathrm{u} \in \{1.6\,\mathrm{s}, 3.2\,\mathrm{s}, 4.8\,\mathrm{s}, 6.4\,\mathrm{s}\}$ serve as reference simulations. For each process time t_u, 1000 lower-fidelity isothermal forming simulations with varying material parameters (cf. Table 2) are performed. The simulation data is provided as a dataset alongside this publication [11]. The input-output behavior of the simulations are then compared using the variance $\mathrm{Var}(r_\mathrm{w})$ of the r_w time series (cf. Eq. 3) and the correlation $\rho(\Delta u, r_\mathrm{w})$ between the input tool stroke Δu and the output r_w (cf. Eq. 4). The results are summarized in Fig. 4. Green crosses represent the high-fidelity thermomechanical simulations, while black dots represent the lower-fidelity isothermal simulations with varied material parameters. Deep black regions indicate a high density of points, while lighter gray regions indicate lower point densities.

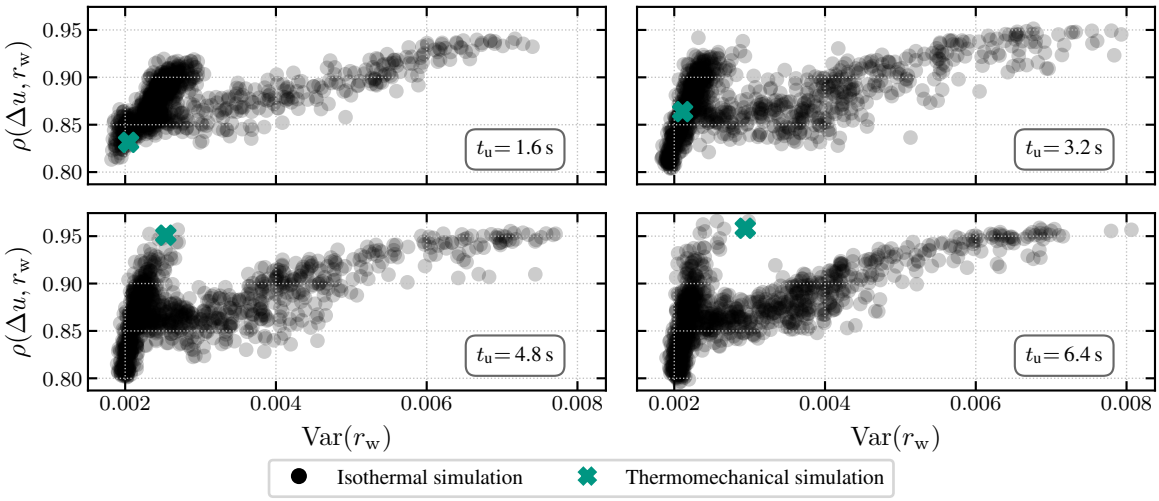

Fig. 4: Validation metrics for thermomechanical and isothermal forming simulations at varying total process times t_u. For isothermal cases, material parameters are varied as in Table 2.

At $t_\mathrm{u} = 1.6\,\mathrm{s}$, the lower-fidelity simulations form a dense cluster at low variance values $\mathrm{Var}(r_\mathrm{w})$, with a smaller number of points extending toward higher variance and correlation values $\rho(\Delta u, r_\mathrm{w})$. As the process time increases, the cluster becomes less compact and spreads toward higher variance and correlation values. This trend indicates that wrinkling behavior is highly sensitive to process time, which influences the deformation rate and thereby the viscosity of the thermoplastic matrix material due to its shear-thinning behavior (Eq. 7). For short total process times $t_\mathrm{u} \in \{1.6\,\mathrm{s}, 3.2\,\mathrm{s}\}$, the high-fidelity thermomechanical simulations fall within the dense clusters of the lower-fidelity isothermal simulations. This suggests that temperature-driven effects are of minor relevance under these conditions because short total process times t_u result in limited cooling of the blank and thereby limiting the significance of reduced temperature-driven phenomena during forming. Analysis of the high-fidelity data shows that the blank temperature remains above $T > 200°\mathrm{C}$ for most of the forming process, with crystallization confined to small regions near the tool contact areas. Since crystallization effects occur only at the final stages of tool stroke u_tool and remain spatially limited, their impact on overall wrinkling behavior is minimal. Consequently, the isothermal model can reproduce the wrinkling behavior of the thermomechanical reference model when its material parameters are properly calibrated. According to the proposed validation framework, the isothermal model does not need to be rejected for these short total process times t_u which is in line with the physical considerations discussed above.

For longer total process times $t_\mathrm{u} \in \{4.8\,\mathrm{s}, 6.4\,\mathrm{s}\}$, the thermomechanical simulations exhibit higher variance and correlation values, deviating from the clusters of the isothermal simulations (cf. Fig. 4). This indicates that the isothermal model fails to reproduce the wrinkling behavior predicted by the thermomechanical reference. Analysis of the high-fidelity simulation data reveals that for these longer total

process times t_u, the blank temperature decreases earlier in the forming process, leading to pronounced thermomechanical coupling effects. In particular, for $t_\mathrm{u} = 6.4\,\mathrm{s}$, regions in tool contact become fully crystallized at a relative tool stroke of $\Delta u \approx 0.55$ (cf. Fig. 3b), resulting in a substantial increase in stiffness and viscosity due to the phase transition of the thermoplastic matrix material from the molten to the solid state (cf. Eq. 9). As significant deformation still occurs after this transition, the wrinkling behavior is strongly influenced by these effects. By the end of the forming process ($\Delta u = 1$), large portions of the blank have crystallized for both $t_\mathrm{u} = 4.8\,\mathrm{s}$ and $t_\mathrm{u} = 6.4\,\mathrm{s}$. It can be concluded that at longer total process times t_u, thermomechanical coupling and phase transitions play a decisive role in the wrinkling behavior, which the isothermal model cannot capture. As the covariance-based metrics of variance and correlation for the isothermal simulations do not overlap with those of the thermomechanical reference (cf. Fig. 4), the isothermal model must be rejected for these conditions. This finding aligns with the physical considerations discussed above.

The number of simulations required for model interrogation is not fixed and was chosen here to demonstrate the framework. In practice, fewer simulations may be sufficient, and simplified characterization or benchmark cases that capture the dominant physical mechanisms can be used instead of complex part geometries. Similarly, the framework does not require a large number of experimental tests. A limited number of representative, time-resolved experimental input-output series can be compared to an ensemble of model predictions to assess whether the relevant system dynamics are captured.

4. Conclusion and Outlook

In this work, a model validation framework was adapted and applied to both one-dimensional rheological models and finite element simulations of thermoforming thermoplastic composite materials. Applying the validation framework to one-dimensional rheological models showed that isothermal models become insufficient when thermal effects are significant, confirming the framework's capability to assess model validity in mechanical contexts. These insights were then transferred to complex finite element simulations, where the validity of an isothermal material model was evaluated against a fully coupled thermomechanical reference. A curvature-based method was introduced to quantitatively evaluate wrinkling severity also considering the natural curvature imposed by the tool geometry. The results showed that the isothermal approach becomes invalid for long total process times with pronounced thermal effects. However, for short total process times, the isothermal model was found to capture the system dynamics adequately, suggesting that with properly chosen material parameters, the lower-fidelity model can be sufficient.

The study demonstrated the versatility of the validation framework for both simplified and complex simulation scenarios, providing objective criteria for assessing model validity based on dynamic behavior rather than point-wise accuracy, and without prior calibration. Future work will apply the framework to experimental data from characterization and application stages to evaluate model validity throughout the virtual design process and to accelerate material model selection. Although the proposed wrinkle evaluation metric r_w effectively quantifies wrinkling severity, it simplifies complex three-dimensional phenomena and depends solely on simulated curvature data, which may limit experimental application. A more sophisticated metric for quantifying wrinkling than a threshold-based approach may capture more detailed characteristics of wrinkling. Further work should refine the metric to capture more detailed and localized wrinkling characteristics and integrate real manufacturing data to enhance the framework's robustness and practical relevance for material model selection in virtual process design. Additionally, exploring the definition of a distance measure in a covariance-based metric space relative to an experimentally obtained system response could facilitate automated model selection and parameter optimization.

Acknowledgments

This work is part of the DFG AI Research Unit 5339 (project no.459291153) and the DFG-funded Heisenberg project "Digitalization of fiber-reinforced polymer processes for resource-efficient manufacturing of lightweight components" (project no. 455807141), which are both funded by the Deutsche Forschungsgemeinschaft, Germany (DFG, German Research Foundation).

Data availability

The simulation data for the isothermal forming simulations used in this work is provided alongside this publication [11] and can be accessed at `https://doi.org/10.5281/zenodo.17977470`.

References

[1] Philippe Boisse, Remko Akkerman, Pierpaolo Carlone, Luise Kärger, Stepan V. Lomov, and James A. Sherwood. Advances in composite forming through 25 years of ESAFORM. *International Journal of Material Forming*, 15(3):99, January 2022. ISSN 1960-6214. doi: 10.1007/s12289-022-01682-8.

[2] Richard M. Vogel and A. Sankarasubramanian. Validation of a watershed model without calibration. *Water Resources Research*, 39(10), January 2003. ISSN 00431397. doi: 10.1029/2002WR001940.

[3] Annie Visser-Quinn, Lindsay Beevers, and Sandhya Patidar. Replication of ecologically relevant hydrological indicators following a modified covariance approach to hydrological model parameterization. *Hydrology and Earth System Sciences*, 23(8):3279–3303, August 2019. ISSN 1027-5606. doi: 10.5194/hess-23-3279-2019.

[4] Dominik Dörr, Fabian J. Schirmaier, Frank Henning, and Luise Kärger. A viscoelastic approach for modeling bending behavior in finite element forming simulation of continuously fiber reinforced composites. *Composites Part A: Applied Science and Manufacturing*, 94:113–123, January 2017. ISSN 1359835X. doi: 10.1016/j.compositesa.2016.11.027.

[5] Dominik Dörr, Tobias Joppich, Daniel Kugele, Frank Henning, and Luise Kärger. A coupled thermomechanical approach for finite element forming simulation of continuously fiber-reinforced semi-crystalline thermoplastics. *Composites Part A: Applied Science and Manufacturing*, 125, January 2019. ISSN 1359835X. doi: 10.1016/j.compositesa.2019.105508.

[6] M. D. McKay, R. J. Beckman, and W. J. Conover. A Comparison of Three Methods for Selecting Values of Input Variables in the Analysis of Output from a Computer Code. *Technometrics*, 21 (2):239–245, 1979. ISSN 0040-1706. doi: 10.2307/1268522.

[7] Siyuan Chen, Adam J. Thompson, Tim J. Dodwell, Stephen R. Hallett, and Jonathan P. H. Belnoue. Fast optimisation of the formability of dry fabric preforms: A Bayesian approach. *Materials & Design*, 230:111986, June 2023. ISSN 0264-1275. doi: 10.1016/j.matdes.2023.111986.

[8] Dominik Dörr, Markus Faisst, Tobias Joppich, Christian Poppe, Frank Henning, and Luise Kärger. Modelling Approach for Anisotropic Inter-Ply Slippage in Finite Element Forming Simulation of Thermoplastic UD-Tapes. In *AIP Proceedings of the 21th International ESAFORM Conference on Material Forming*, January 2018.

[9] Dominik Dörr, Daniel Kugele, Tobias Joppich, Frank Henning, and Luise Kärger. On the relevance of thermomechanics and crystallization kinetics for FE thermoforming simulation of semi-crystalline thermoplastic tapes. In *Proceedings of the 22nd International ESAFORM Conference on Material Forming: ESAFORM 2019*, page 020011, Vitoria-Gasteiz, Spain, 2019. doi: 10.1063/1.5112516.

[10] Georg Zeeb, Johannes Mitsch, Michael Wilhelm, Luise Kärger, and Frank Henning. Influence of gripper positions on the formation of wrinkles during the thermoforming process of thermoplastic UD-tape laminates. In *Materials Research Proceedings*, volume 54, pages 544–553. Materials Research Forum LLC, 2025. doi: 10.21741/9781644903599-59.

[11] Johannes Mitsch and Luise Kärger. Process simulation data for thermoforming of continuous fiber-reinforced composite materials, Zenodo, December 2025.

[12] Chen-shi Dong and Guo-zhao Wang. Curvatures estimation on triangular mesh. *Journal of Zhejiang University-SCIENCE A*, 6(S1):128–136, January 2005. ISSN 1673-565X. doi: 10.1631/jzus.2005.AS0128.

The publication of this article was funded by the Karlsruhe Institute of Technology 10.13039/100009133